Journal Pre-proof

An epidermal-specific role for arginase1 during cutaneous wound repair.

Rachel A. Crompton, Helen Williams, Laura Campbell, Hui Kheng Lim, Charis Saville, David M. Ansell, Adam Reid, Jason Wong, Leah A. Vardy, Matthew J. Hardman, Sheena M. Cruickshank

PII: S0022-202X(21)02288-0

DOI: https://doi.org/10.1016/j.jid.2021.09.009

Reference: JID 3139

To appear in: *The Journal of Investigative Dermatology*

Received Date: 23 April 2021

Revised Date: 3 September 2021

Accepted Date: 10 September 2021

Please cite this article as: Crompton RA, Williams H, Campbell L, Lim HK, Saville C, Ansell DM, Reid A, Wong J, Vardy LA, Hardman MJ, Cruickshank SM, An epidermal-specific role for arginase1 during cutaneous wound repair., *The Journal of Investigative Dermatology* (2021), doi: https://doi.org/10.1016/j.jid.2021.09.009.

Title: An epidermal-specific role for arginase1 during cutaneous wound repair.

Authors and affiliations:

Rachel A. Crompton (0000-0001-5878-9292)[1*], Helen Williams (0000-0001-5723-501X)[1*], Laura Campbell (0000-0001-8888-3917)[1], Lim Hui Kheng (0000-0002-3510-5334)[2], Charis Saville[1] (0000-0002-6796-001X), David M. Ansell (0000-0002-6977-4288)[1,4], Adam Reid (0000-0003-1752-3302)[1], Jason Wong (0000-0003-2592-3226)[1], Leah A. Vardy (0000-0003-4186-684X)[2], Matthew J. Hardman (0000-0002-6423-5074)[3] and Sheena M. Cruickshank (0000-0002-3047-5475)[1].

[1] Lydia Becker Institute of Immunology and Inflammation, Manchester Academic Health Science Centre, Faculty of Biology, Medicine and Health, University of Manchester, Oxford Road, Manchester, M13 9PT, United Kingdom.

[2] Skin Research Institute of Singapore, A*STAR, 8 Biomedical Grove, Singapore 138648, Singapore.

[3] Centre for Atherothrombosis and Metabolic Disease, Hull York Medical School, The University of Hull, Cottingham Road, Hull, HU6 7RX, United Kingdom.

[4] School of Chemistry and Bioscience, University of Bradford, Bradford, West Yorkshire, BD7 1DP, United Kingdom.

*Authors contributed equally to the study.

CORRESPONDING AUTHOR:

Prof Sheena M. Cruickshank

Address : Faculty of Biology, Medicine and Health. AV Hill Building. Oxford Road. The University of Manchester. Manchester. M13 9PT.

Email : sheena.cruickshank@manchester.ac.uk. Phone : +44 (0)161 275 1578

ABBREVIATIONS: [AMD1] (S-adenosylmethionine decarboxylase proenzyme), [ARG1] (Arginase1), [DFUs] (Diabetic foot ulcers), [Nor-NOHA] (Nomega-hydroxy-nor-L-arginine), [NOS] (Nitric Oxide Synthase, [OAT] (Ornithine amino transferase), [ODC] (Ornithine decarboxylase), [ovx] (ovariectomized)

ABSTRACT

Non-healing wounds are a major area of unmet clinical need remaining problematic to treat. Improved understanding of pro-healing mechanisms is invaluable. The enzyme arginase1 is involved in pro-healing responses with its role in macrophages best characterized. Arginase1 is also expressed by keratinocytes; however, arginase1 function in these critical wound repair cells is not understood. We characterized arginase1 expression in keratinocytes during normal cutaneous repair and reveal *de novo* temporal and spatial expression at the epidermal wound edge. Interestingly, epidermal arginase1 expression was decreased in both human and murine delayed healing wounds. We therefore generated a keratinocyte specific arginase1-null mouse model (*K14-cre;Arg1*$^{fl/fl}$) to explore arginase function. Wound repair, linked to changes in keratinocyte proliferation, migration and differentiation, was significantly delayed in *K14-cre;Arg1*$^{fl/fl}$ mice. Similarly, using the arginase inhibitor nor-NOHA, human *in vitro* and *ex vivo* models further confirmed this finding, revealing the importance of the downstream polyamine pathway in repair. Indeed, restoring the balance in arginase1 activity via addition of putrescine, proved beneficial in wound closure. In summary, we demonstrate that epidermal arginase1 plays a, to our knowledge, previously unreported intrinsic role in cutaneous healing, highlighting epidermal arginase1 and downstream mediators as potential targets for the therapeutic modulation of wound repair.

INTRODUCTION

Non-healing wounds including pressure, diabetic, venous ulcers and non-healing surgical wounds, are a significant health burden (Harding et al., 2002), characterized by excessive inflammation and defective re-epithelialization. Numerous factors have been implicated in defective wound healing, including altered levels of the arginine metabolic enzyme, arginase1. Arginine metabolism is involved in numerous processes including; immune regulation (Bronte and Zanovello, 2005, Tong and Barbul, 2004); the Krebs cycle; the urea cycle; growth hormone secretion; cell proliferation (Bronte et al., 2003, Li et al., 2002, Ochoa et al., 2001, Pegg and McCann, 1982) and collagen synthesis (Barbul, 2008). The effect on these processes depends on how L-arginine is metabolized and the balance of the competitive arginine catabolic enzymes- nitric oxide synthase (NOS) and arginase1. NOS metabolism of arginine leads to citrulline and nitric oxide (NO) production - important in the early pro-inflammatory phase of repair, including anti-microbial effects and cell death. In contrast, arginase1 metabolism of arginine has two primary functions; detoxification of ammonia via the urea cycle and production of ornithine, which is known to be critical for the pro-healing response. Ornithine decarboxylase (ODC) metabolism of ornithine leads to polyamine synthesis (putrescine, spermidine and spermine), involved in epithelial stem cell function, cell proliferation and differentiation (Pietila et al., 2005, Ramot et al., 2011). Alternatively, ornithine amino transferase (OAT) metabolism of ornithine, promotes proline production, involved in collagen synthesis (Jenkinson et al., 1996, Witte et al., 2002). Thus, multiple facets of arginase1 activity are linked with the repair response.

Conflicting reports of arginase's impact on healing are likely due to its involvement in many aspects of the healing response. Dysregulation of arginase and pathway components are observed in diabetes (Kovamees et al., 2016, Ramírez-Zamora et al., 2013), advanced age

(Kim et al., 2009, Ming and Yang, 2013, Moretto et al., 2019, Muller et al., 2008), chronic wounds and delayed healing (Abd-El-Aleem et al., 2000, Jude et al., 1999, Sindrilaru et al., 2011). Down-regulation of *ARG1* gene expression has been linked to age-associated human (Hardman and Ashcroft, 2008) and murine delayed healing (Campbell et al., 2013); conversely, increased arginase activity was reported in diabetic wounds (Kampfer et al., 2003). Similarly, mechanistic mouse studies report conflicting effects on wound repair showing both improved (Kavalukas et al., 2012) and delayed healing (Campbell et al., 2013) when arginase activity was inhibited either globally or in macrophages. Thus, although it is clear arginase plays a major role in wound healing, further investigation into the role of arginase1 in cutaneous repair is needed. Indeed, the apparent discrepancies between published studies suggest cell and wound-type specific roles in healing.

Arginase1 is best characterized in activated 'anti-inflammatory' (M2) macrophages, and studies on cutaneous arginase1 function is almost exclusively confined to its role in macrophages (Mahdavian Delavary et al., 2011). Arginase1 is however, also expressed in other prominent wound cell types including keratinocytes (Bruch-Gerharz et al., 2003). On cutaneous wounding the keratinocytes at the wound edge proliferate and migrate during re-epithelialization to close the wound and these processes are frequently impaired in chronic wounds. In normal healing, keratinocytes will then differentiate to stratify the newly formed epidermis, releasing factors such as lipids, cytokines and anti-microbial products to restore skin barrier integrity and contribute to immune defence (Coulombe, 1997, Pastar et al., 2014). Although arginase1 has been implicated in functions associated with epidermal repair, the role of epidermal arginase1 is poorly understood. Moreover, the functional relevance of arginase1 in epidermal keratinocytes, especially in cutaneous healing, is largely unexplored.

This study aimed to determine the epidermal specific role of arginase1 in cutaneous wound repair. We hypothesized that, keratinocyte specific defects in arginase1 function, contribute to pathological healing. To test this hypothesis, we determined epidermal arginase1 expression profiles in human and murine delayed healing models and developed a keratinocyte-specific arginase1 null mouse.

RESULTS AND DISCUSSION

Epidermal arginase1 is temporally induced during cutaneous healing

To define the role of epidermal arginase1 in cutaneous healing we characterized temporal and spatial arginase expression in wound edge keratinocytes during acute wound repair using immunohistochemical (IHC) analysis (Figure 1). Low arginase1 expression was observed in the unwounded epidermis (Supplementary Figure S1); however, expression was high at the wound edge and peri-wound epidermis, specifically the suprabasal layers of the wound edge epidermis, of both human (Figure 1a) and murine (Figure 1b) acute wounds. Arginase1 immunofluorescence (IF) analysis of murine acute wounds, showed low arginase1 wound epidermal expression at 1day post-wounding (indicated by co-localization with keratin14 (K14)). By day 3, arginase1 was highly induced in the suprabasal layers of the neo-epidermis and peri-wound epidermis. Expression remained high at day 5, but almost completely disappeared by day 7 and was undetectable at 14days post-wounding, when the hyperproliferative wound epidermis had almost completely resolved (Figure 1c, d). Interestingly, this expression pattern of epidermal arginase during the proliferative, inflammatory and remodelling stages of cutaneous repair suggests multiple roles in healing.

Epidermal arginase1 expression is reduced in delayed healing wounds

Arginase1 was assessed in human chronic wounds; ovariectomized (ovx) and age-matched intact controls (Emmerson et al, 2012); and aged murine models of delayed healing. In murine delayed healing wounds (ovx and aged) arginase1 was significantly reduced at 3days post-wounding compared to intact and young (7week old) controls, respectively (Figure 2a-d, Supplementary Figure S2). This finding was mirrored in human chronic DFUs whereby, arginase1 expression was reduced at initial clinical presentation in wounds that failed to heal within 12weeks, compared to those that healed within 8weeks of clinical assessment (Figure 2e-g). The distinct localization in acute wounds contrasted with arginase1 expression observed throughout the epidermis in DFUs (Figure 2f,g), perhaps more akin to increased levels of global arginase typically reported in chronic wounds (Abd-El-Aleem et al., 2000, Jude et al., 1999, Wessagowit et al., 2004). These findings appear to contradict previous work demonstrating heightened arginase1 expression throughout the epidermis in chronic venous leg ulcers (Abd El-Aleem et al., 2020). One explanation for this is that the published data compared epidermal arginase expression at the ulcer edge with normal epidermis away from the ulcer edge. Alternatively, these observations may reflect the arginase1 expression we observed in DFUs that subsequently healed (Figure 2), illustrating the importance of longitudinal sampling where possible. Nevertheless, our data implicate dysregulation of epidermal arginase1 in defective healing. Future studies could explore this dynamic expression using diabetic models such as the db/db mouse, to further our understanding.

Epidermal specific deletion of arginase1 delays acute murine healing

We made a keratinocyte specific arginase1 knockout mouse model (*K14cre;Arg1*$^{fl/fl}$). To confirm the depletion we performed PCR (Supplementary Text), arginase assay and IHC Figure 3). Collectively these protocols confirmed the efficacy of the epidermal arginase1

depletion and critically the specificity of depletionwhilst retaining dermal arginase1 expression (Figure 3a). Furthermore, the observation of reduced global arginase activity (Figure 3b), implicates keratinocytes as a major source of arginase1 during repair. Histological characterization showed the skin of unwounded *K14cre;Arg1*$^{fl/fl}$ mice appeared akin to cre controls in most parameters assessed including H+E, keratin14, 10 and 6, proliferation and apoptosis, with the exception of loricrin, which was reduced in *K14cre;Arg1*$^{fl/fl}$ unwounded skin (Supplementary Figure S3).

We observed an overall delay in healing in the *K14cre;Arg1*$^{fl/fl}$ mice compared to cre controls. Histo-morphometric quantification of wound area demonstrated significantly larger wounds (Figure 3c, d), an altered immune response and immune cell composition (Supplementary Figure S4) and significantly reduced re-epithelialization at 3days post-wounding (Figure 3e, f) in the *K14cre;Arg1*$^{fl/fl}$ wounds compared to controls, which was recapitulated *in vitro* (Supplementary Figure S5). These results demonstrate that epidermal arginase1 is important for timely cutaneous wound repair, impacting both dermal and epidermal responses.

To determine how arginase1 influences healing, a microarray of laser capture micro-dissected, 3day neo-epidermal wound tissue was performed. The most significant gene alterations observed in the *K14cre;Arg1*$^{fl/fl}$ wounds compared to control were associated with decreased cell-cycle progression and cell viability (Figure 3g). Changes in genes associated with an altered immune response were also identified, including cytokines, chemokines and host microbial response genes (Supplementary Figure S4d-f). Given the marked effects of arginase1 deletion on re-epithelialization we investigated arginase1 in keratinocyte proliferation and differentiation.

Arginase1 is required for effective regulation of keratinocyte proliferation

Upon injury, keratinocytes become activated, priming cells to proliferate and migrate to seal the open wound. Microarray data implicated proliferation and cell-cycle progression as being impacted in the absence of keratinocyte arginase. *In vivo* wounds showed the absence of keratinocyte arginase1, in *K14cre;Arg1*$^{fl/fl}$ mice, resulted in reduced activation and proliferation of keratinocytes at 3days post-wounding (Figure 4). Quantification of keratin6 (K6) staining (Figure 4a-c), a marker of hyper-proliferation and keratinocyte 'activation', demonstrated a significantly reduced distance of K6 expression extending from the wound edge at 3days post-wounding compared to cre controls (Figure 4b). Similarly, there was a significant reduction of expression of the proliferation marker, Ki67 (Figure 4d) in the neo-epidermis (Figure 4e) and basal keratinocytes (Figure 4f), observed specifically at the wound edge (Figure 4g), with a lesser effect observed extending to the peri-wound epidermis (Figure 4h) in *K14cre;Arg1*$^{fl/fl}$ compared to cre controls at 3days post-wounding.

. Our findings are supported in a recent paper that showed localization of epidermal arginase1 in proliferative keratinocytes in skin remote to the wound edge and throughout the epidermis at the ulcer edge in chronic venous leg ulcers (Abd El-Aleem et al., 2020). Our analysis of DFUs (Figure 2e-g) showed similar results with arginase1 expression throughout the epidermis implying a role for arginase1 in the hyperproliferative epidermal phenotype of chronic wounds.

A lack of epidermal arginase1 delays keratinocyte stratification

Regulation of epidermal proliferation and differentiation are interlinked and during re-epithelialization keratinocytes away from the leading edge stop proliferating and start to differentiate, to stratify the newly formed epidermis. Interestingly, arginase1 expression was

high in the differentiated suprabasal wound edge epidermal keratinocytes *in vivo* (Figure 1 and 5a) and the differentiation marker loricrin, in *K14cre;Arg1*$^{fl/fl}$, was decreased in unwounded skin (Supplementary Figure S3). Furthermore, during acute wound repair the suprabasal arginase1 expression in the neo-epidermis was co-localized with differentiation markers keratin 10, filaggrin and loricrin (Figure 5a). *ARG1* mRNA levels were also increased upon *in vitro* differentiation of keratinocytes to a similar level as *KRT10, FLG* and *LOR* (Figure 5b), suggesting a possible role for arginase in epidermal differentiation. Indeed, other studies have shown that K10 and profillagrin contain high levels of arginine residues and during epidermal remodelling these proteins undergo deamination which produces citrulline and releases free amino acids including arginine (Mechin et al., 2007) - the substrate for arginase. Citrulline is both a product of L-arginine metabolism by NOS and a substrate for L-arginine *de novo* synthesis (Wu and Morris, 1998), therefore providing greater levels of arginine substrate in differentiating cells which could explain elevated arginase1 levels. Arginase1 may also act as a precursor to keratinocyte differentiation as arginase1 metabolic products such as proline are major components of cornified envelope proteins (Hohl et al., 1995) and polyamines are required for keratinocyte differentiation (Anisa B. Rahim, 2021). Indeed, IHC analysis of the differentiation associated markers K10 and loricrin in acute mouse wounds (Figure 5c), demonstrated significantly reduced epidermal differentiation by 7days post-wounding in *K14cre;Arg1*$^{fl/fl}$ wounds compared to control with reduced loricrin (Figure 5d, e), a major differentiation associated cornified envelope protein (Kalinin et al., 2002, Koch et al., 2000). Loricrin was also reduced in unwounded skin of *K14cre;Arg1*$^{fl/fl}$ mice (Supplementary Figure S3). Notably, hyperkeratosis and parakeratosis are characteristic of chronic wound keratinocytes (Stojadinovic et al., 2005), due to dysregulation of differentiation (Stojadinovic et al., 2008). Collectively, these results support a role for arginase1 as a precursor to epidermal differentiation during repair, also suggesting

altered epidermal arginase levels impact normal differentiation and the chronic wound phenotype.

Manipulating the balance of arginase activity restores healing in human models of cutaneous repair

Arginase1 metabolizes Arginine into ornithine, a precursor to proline or putrescine, required for the synthesis of polyamines, spermidine and spermine (Latour et al., 2020). Decreased arginase will lead to depletion of putrescine and polyamines, known to be important for wound healing. Polyamine levels and regulators of polyamine production including ODC1 and AMD1 are upregulated at the wound edge (Lim et al., 2018, Maeno et al., 1990, Mizutani et al., 1974, Shi et al., 2002). Spermine and spermidine are essential for cell migration and promote directed migration (Nakajima et al., 2015, Tai et al., 2018) (Lim et al., 2018). To determine if impaired re-epithelialization during wound healing caused by arginase inhibition is a consequence of decreased polyamine levels, we assessed whether putrescine could rescue the wound-healing phenotype. Additon of arginase inhibitor nor-NOHA delayed wound closure in a keratinocyte scratch assay which was rescued with the addition of putrescine (Figure 6a, b). Topical application of nor-NOHA to a human wound explant led to reduced wound re-epithelialization that was also restored with putrescine (Figure c, d). These data suggest that, on wounding, arginase functions, at least in part, to promote putrescine levels which are required for wound closure. However, while supplementation with putrescine rescued the arginase inhibition phenotype, when added in the presence of arginase, putrescine inhibited wound closure in *in vitro* and *ex vivo* models (Figure 6). Similarly, previous reports have demonstrated high putrescine levels inhibit scratch wound closure (Anisa B. Rahim, 2021, Lim et al., 2018). Together these data suggest that arginase plays a crucial role in controlling the levels of putrescine at the wound edge which is required for conversion to the

polyamines spermine and spermidine, which in turn control the balance between proliferation and cell migration. Importantly, the ability to restore the balance in arginase and polyamine activity leading to rescue of the delayed healing response, demonstrates the therapeutic potential in manipulating the arginase pathway for improved healing of chronic wounds.

We propose disparate roles for arginase1 in epidermal remodelling, where timing of expression is key to determining healing outcome. This is supported by the expression profile of epidermal arginase1 observed during acute healing, whereby arginase1 is upregulated (D3-7 post-wounding) when epidermal remodelling, including proliferation and migration are at their peak. Furthermore, wound analysis showed heightened epidermal keratinocyte activation at 7days post-wounding in *K14cre;Arg1*$^{fl/fl}$ acute wounds compared to cre controls. Such observations suggest a late proliferative response, concomitant to a delay in the early keratinocyte epidermal response, implicating a compensation mechanism. Indeed this lack of early keratinocyte arginase response, followed by an extended late response, corresponds to the typical chronic wound epidermal phenotype, that is hyperproliferative yet non-migratory. Thus, the timing of arginase induction in keratinocytes may be critical in eliciting an early wound response, with epidermal arginase levels potentially being a predetermining factor of healing outcome. As heightened arginase1 expression was more localized to the suprabasal layers of the peri-wound and neo-epidermis it seems unlikely that it directly influences proliferation at the wound edge. High levels of arginase indicate high levels of putrescine, which in turn is typically converted to spermidine and spermine (Supplementary Figure S6). When spermidine and spermine levels are too high they are either converted back to putrescine or spermidine with the release of $H_20_{2,}$ or are acetylated and secreted (Wallace and Mackarel, 1998). Thus, we would suggest that epidermal arginase influences proliferation *in vivo* via the secretion of polyamines from suprabasal arginase high expressing cells. The

polyamines could act directly by extracellular polyamine influx into basal proliferating cells, and/or indirectly via the impact of polyamines altering epidermal and/or dermal specific immune responses (Lou et al., 2020).

Collectively, our data demonstrates a positive correlation between early arginase1 expression and healing outcome, consistent across multiple models of both murine and human cutaneous healing. We also revealkeratinocyte-specific roles for arginase1 in wound cellular proliferation, migration and differentiation. We note that these processes are frequently dysregulated in chronic wounds, positioning the epidermal arginase1 pathway as an exciting target for therapeutic modulation to promote wound repair.

MATERIALS AND METHODS

Full details are given in Supplementary Text linked to the online version.

Human acute and chronic wounds

Clinical investigation was conducted according to the Declaration of Helsinki principles. Human studies were approved by the University of Manchester's Research Ethics Committee (REC) under 07/Q1406/14 or 13/SC/0499 REC approval, and with written informed consent. Acute wound 1.5 mm punch biopsies were collected from 3 healthy volunteers (male, aged ≥30 years) (Thomason et al., 2012). Chronic wound biopsy samples from 19 patients (mixed sex, aged ≥40 years) with chronic DFU (Williams et al., 2018). *Ex vivo* methodology culture of skin wound explants was adapted from (Stojadinovic and Tomic-Canic, 2013) and via communication with Dr David Ansell.

Murine wounding

Animal studies were conducted according to the Animals (Scientific Procedures) Act 1986 under project licences 70/8136 and 40/3713 approved by the UK Home Office. A keratinocyte specific arginase1-null mouse model (*K14-cre;Arg1*$^{fl/fl}$) was generated for this study (see supplemental methods online). 8 week old female *K14-cre;Arg1*$^{fl/fl}$, *K14-cre;Arg1*$^{+/+}$ (wild-type controls), female C57BL/6J 6-8week old (young), 18month old (aged) or 10-week ovariectomised (bilateral ovariectomy performed 3 weeks before wounding) mice received two 1cm full-thickness dorsal incisions and left to heal by secondary intention (Ashcroft et al., 2003, Emmerson et al., 2012). Tissue harvest was performed at 1, 3, 5, 7 and 14days post-wounding.

Histology and immunohistochemistry

Histological sections were prepared as (Campbell et al., 2013). Briefly, paraffin embedded sections were stained with H+E or subjected to IHC or IF analyses against the following markers; arginase, NOS2, keratin6, kertain14, loricrin, keratin10, filaggrin, Ki67, Neutrophil, Mac3 (Supplementary Table S1).

For IHC, antibody staining was detected using the Vector Elite ABC Kits (Rabbit, Rat, Goat) visualized with NOVA Red and IF stained sections were visualized using fluorescent secondaries (donkey anti-goat AF594; donkey anti-rabbit AF488; Abcam, Cambridge, UK,), counterstained with DAPI (ThermoFisher Scientific, Loughborough, UK). TUNEL staining was performed using the i*n Situ* Cell Death Detection Kit Fluorescein (Roche, Welwyn Garden City, UK) according to manufacturers' instructions. Analysis was performed blinded by two independent investigators. Refer to Supplementary text for details on analytical methods performed for each stain.

Arginase activity assay

Total wound arginase activity was assessed by the quantification of urea production via the metabolizm of L-arginine by arginase, modified from (Corraliza et al., 1994). To normalize the samples, the protein concentration in cell lysates was measured using a BCA Protein Assay Kit. (ThermoFisher Scientific).

Microarray

Laser Capture Microdissection (LCM) was used to isolate neo-epidermis cells from 3day incisional wounds. RNA was isolated using the RNAqueous-Micro Kit (AM1931; Ambion, Loughborough, UK) as per manufacturer's instructions. RNA samples isolated by LCM from

frozen wound sections, were processed by the Genomic Technologies Core Facility in the Faculty of Biology, Medicine and Health, University of Manchester, for microarray analysis, using the mouse Clariom D Assay (Applied Biosystems).

***In vitro* cell analysis**

Keratinocyte culture

Normal human epidermal keratinocytes (NHEKs) isolated from juvenile foreskin (Promocell) were cultured in keratinocyte growth medium 2 (Promocell) at 37°C with 5% CO_2. NHEKs were used in experiments at P3-5. N/TERT-1 cells were cultured at 37°C with 5% CO_2 in Keratinocyte Serum Free Media as previously described (Lim et al., 2018) and transferred to DFK-2 media and K-SFM, all from GIBCO). HaCaT cells (ATCC12191) were cultured in DMEM (high glucose) with 10% FBS and 1x Pen/Strep at 37°C with 5% CO_2.

Keratinocyte scratch assay

HaCaT cells were seeded into 24well plates, cultured until confluent, then scatched with a 1ml sterile pipette tip. 0hr controls were immediately stained with crystal violet, while nor-NOHA or untreated wells were incubated for 24hrs before staining. Three images/well were captured using a Nikon Eclipse E600 microscope and SPOT insight camera (Image solutions Inc, Preston, UK). An average of 5 measurements/image from 3 images/well were used to calculate percentage wound width remaining using Image Pro Plus software (Media Cybernetics, Abingdon, UK). N/TERT-1 cells seeded at a density of $1x10^4$ cells/well incubated for 3days in Keratinocyte Serum Free Media, 2days in DFK-2 before treatment with nor-NOHA 5µM (Cayman, Michigan, USA) or Putrescine 10µM (Sigma) in DFK-2 for 24 or 48hrs prior to scratch. Confluent monolayers were scratched with an Essen wound maker, rinsed with sterile PBS and DFK-2 media with or without nor-NOHA/putrescine was

added and cells were imaged every 2hr with the Incucyte system. Assay was performed in biological triplicate. Percentage wound closure was calculated based on scratch width after the specified duration, relative to initial width.

Differentiation assay

NHEKs were seeded into 6well plates at $4x10^5$ cells/well. At ~60% confluence, cells were transitioned over 2days into CNT-PR culture media, prior to switching to defined differentiation media CNT-PR-D (CellnTech). Cells were collected before the switch and 2, 4, and 6days after.

Quantitative real-time PCR

Total RNA was isolated from NHEKs by Trizol/Chloroform extraction and column based purification using the Purelink RNA mini kit (Invitrogen, Paisley, UK).

Statistical analysis

Ordinary or repeated measures two-way ANOVA followed by Sidak's multiple comparisons test was performed for all grouped data with two factors (1. genotype/treatment and 2. time) and adjusted P values reported. If normality could not be assumed, statistical comparisons between groups was determined using the Mann-Whitney test at each timepoint and the two-tailed P value reported. Ordinary one-way ANOVA was used for single factor data with 3 or more groups followed by Tukey's multiple comparisons; or Kruskal Wallis test with Dunn's multiple comparisons if normality could not be assumed. Single factor data with less than 3 groups were analyzed using the unpaired t-test and the two-tailed P value reported. All analysis was performed using GraphPad Prism 8 Version 8.4.2 (GraphPad Software, Inc. CA, USA). A probability value of less than 0.05 was considered statistically significant.

DATA AVAILABILITY STATEMENT

Datasets related to this article can be found at https://www.ebi.ac.uk/arrayexpress/, hosted at ArrayExpress (accession number: E-MTAB-10213).

ORCID IDs

Rachel A. Crompton (0000-0001-5878-9292), Helen Williams (0000-0001-5723-501X), Laura Campbell (0000-0001-8888-3917), Lim Hui Kheng (0000-0002-3510-5334), Charis Saville (0000-0002-6796-001X), David M. Ansell (0000-0002-6977-4288), Adam Reid (0000-0003-1752-3302), Jason Wong (0000-0003-2592-3226), Leah A. Vardy (0000-0003-4186-684X), Matthew J. Hardman (0000-0002-6423-5074) and Sheena M. Cruickshank (0000-0002-3047-5475).

CONFLICT OF INTEREST: The authors have declared no conflicts of interests.

ACKNOWLEDGMENTS

The work was funded by a MRC MICA project grant awarded to SC and MH and a BBSRC PhD awarded to SC, RC. We acknowledge the support of Dr Cath Booth and Dr James Wilson of Epistem Ltd. for their support and use of their facilities for this study. The histological sample processing was performed using the Histology Core Facility equipment. The Bioimaging Facility microscopes used in this study were purchased with grants from BBSRC, Wellcome and the University of Manchester Strategic Fund. Special thanks go to Roger Meadows and Steve Marsden for their help with the microscopy. We acknowledge the support of Andy Hayes and Michal Smiga of the Genomic Technologies Core Facility, in addition to Leo Zeef of the Bioinformatics Core Facility, in the Faculty of Biology Medicine

and Health, University of Manchester, for their contribution towards microarray sample processing and analysis.

AUTHOR CONTRIBUTIONS

Conceptualization: RAC, HW, LC, LAV, MJH, SMC; Methodology: RAC, HW, DMA; Validation: RAC, HW; Formal Analysis: RAC, HW; Investigation; RAC, HW, LC, LHK; Resources; LC, CS, DMA, AR, JW; Writing – Original Draft: RAC, HW, LC, SMC; Writing – Review and Editing: RAC, HW, LC, DMA, JW, LAV, MJH, SMC; Funding acquisition: MJH, SMC; Supervision: SMC.

REFERENCES

Abd-El-Aleem SA, Ferguson MW, Appleton I, Kairsingh S, Jude EB, Jones K, et al. Expression of nitric oxide synthase isoforms and arginase in normal human skin and chronic venous leg ulcers. J Pathol 2000;191(4):434-42.

Abd El-Aleem SA, Abd-Elghany MI, Ali Saber E, Jude EB, Djouhri L. A possible role for inducible arginase isoform (AI) in the pathogenesis of chronic venous leg ulcer. Journal of cellular physiology 2020;n/a(n/a).

Anisa B. Rahim HKL, Christina Yan Ru Tan, Li Jia, Vonny Ivon Leo, Takeshi Uemura, Jonathan Hardman-Smart, John E.A. Common, Thiam Chye Lim, Sophie Bellanger, Ralf Paus, Kazuei Igarashi, Henry Yang, Leah A. Vardy. The polyamine regulator AMD1 up-regulates spermine levels to drive epidermal. Journal of Investigative Dermatology 2021.

Ashcroft GS, Mills SJ, Lei K, Gibbons L, Jeong MJ, Taniguchi M, et al. Estrogen modulates cutaneous wound healing by downregulating macrophage migration inhibitory factor. The Journal of clinical investigation 2003;111(9):1309-18.

Barbul A. Proline precursors to sustain Mammalian collagen synthesis. J Nutr 2008;138(10):2021S-4S.

Bronte V, Serafini P, Mazzoni A, Segal DM, Zanovello P. L-arginine metabolism in myeloid cells controls T-lymphocyte functions. Trends Immunol 2003;24(6):302-6.

Bronte V, Zanovello P. Regulation of immune responses by L-arginine metabolism. Nature reviews Immunology 2005;5(8):641-54.

Bruch-Gerharz D, Schnorr O, Suschek C, Beck KF, Pfeilschifter J, Ruzicka T, et al. Arginase 1 overexpression in psoriasis - Limitation of inducible nitric oxide synthase activity as a molecular mechanism for keratinocyte hyperproliferation. American Journal of Pathology 2003;162(1):203-11.

Campbell L, Saville CR, Murray PJ, Cruickshank SM, Hardman MJ. Local Arginase 1 Activity Is Required for Cutaneous Wound Healing. J Invest Dermatol 2013;133(10):2461-70.

Corraliza IM, Campo ML, Soler G, Modolell M. Determination of arginase activity in macrophages: a micromethod. Journal of immunological methods 1994;174(1-2):231-5.

Coulombe PA. Towards a molecular definition of keratinocyte activation after acute injury to stratified epithelia. Biochemical and biophysical research communications 1997;236(2):231-8.

Emmerson E, Campbell L, Davies FC, Ross NL, Ashcroft GS, Krust A, et al. Insulin-like growth factor-1 promotes wound healing in estrogen-deprived mice: new insights into cutaneous IGF-1R/ERalpha cross talk. J Invest Dermatol 2012;132(12):2838-48.

Harding KG, Morris HL, Patel GK. Science, medicine and the future: healing chronic wounds. Bmj 2002;324(7330):160-3.

Hardman MJ, Ashcroft GS. Estrogen, not intrinsic aging, is the major regulator of delayed human wound healing in the elderly. Genome Biol 2008;9(5):R80.

Hohl D, de Viragh PA, Amiguet-Barras F, Gibbs S, Backendorf C, Huber M. The small proline-rich proteins constitute a multigene family of differentially regulated cornified cell envelope precursor proteins. J Invest Dermatol 1995;104(6):902-9.

Jenkinson CP, Grody WW, Cederbaum SD. Comparative properties of arginases. Comparative biochemistry and physiology Part B, Biochemistry & molecular biology 1996;114(1):107-32.

Jude EB, Boulton AJ, Ferguson MW, Appleton I. The role of nitric oxide synthase isoforms and arginase in the pathogenesis of diabetic foot ulcers: possible modulatory effects by transforming growth factor beta 1. Diabetologia 1999;42(6):748-57.

Kalinin AE, Kajava AV, Steinert PM. Epithelial barrier function: assembly and structural features of the cornified cell envelope. BioEssays : news and reviews in molecular, cellular and developmental biology 2002;24(9):789-800.

Kampfer H, Pfeilschifter J, Frank S. Expression and activity of arginase isoenzymes during normal and diabetes-impaired skin repair. J Invest Dermatol 2003;121(6):1544-51.

Kavalukas SL, Uzgare AR, Bivalacqua TJ, Barbul A. Arginase inhibition promotes wound healing in mice. Surgery 2012;151(2):287-95.

Kim JH, Bugaj LJ, Oh YJ, Bivalacqua TJ, Ryoo S, Soucy KG, et al. Arginase inhibition restores NOS coupling and reverses endothelial dysfunction and vascular stiffness in old rats. Journal of applied physiology 2009;107(4):1249-57.

Koch PJ, de Viragh PA, Scharer E, Bundman D, Longley MA, Bickenbach J, et al. Lessons from loricrin-deficient mice: compensatory mechanisms maintaining skin barrier function in the absence of a major cornified envelope protein. J Cell Biol 2000;151(2):389-400.

Kovamees O, Shemyakin A, Pernow J. Amino acid metabolism reflecting arginase activity is increased in patients with type 2 diabetes and associated with endothelial dysfunction. Diabetes Vasc Dis Re 2016;13(5):354-60.

Latour YL, Gobert AP, Wilson KT. The role of polyamines in the regulation of macrophage polarization and function. Amino Acids 2020;52(2):151-60.

Li H, Meininger CJ, Kelly KA, Hawker JR, Jr., Morris SM, Jr., Wu G. Activities of arginase I and II are limiting for endothelial cell proliferation. American journal of physiology Regulatory, integrative and comparative physiology 2002;282(1):R64-9.

Lim HK, Rahim AB, Leo VI, Das S, Lim TC, Uemura T, et al. Polyamine Regulator AMD1 Promotes Cell Migration in Epidermal Wound Healing. J Invest Dermatol 2018;138(12):2653-65.

Lou F, Sun Y, Xu Z, Niu L, Wang Z, Deng S, et al. Excessive Polyamine Generation in Keratinocytes Promotes Self-RNA Sensing by Dendritic Cells in Psoriasis. Immunity 2020;53(1):204-16 e10.

Maeno Y, Takabe F, Inoue H, Iwasa M. A study on the vital reaction in wounded skin: simultaneous determination of histamine and polyamines in injured rat skin by high-performance liquid chromatography. Forensic Sci Int 1990;46(3):255-68.

Mahdavian Delavary B, van der Veer WM, van Egmond M, Niessen FB, Beelen RH. Macrophages in skin injury and repair. Immunobiology 2011;216(7):753-62.

Mechin MC, Sebbag M, Arnaud J, Nachat R, Foulquier C, Adoue V, et al. Update on peptidylarginine deiminases and deimination in skin physiology and severe human diseases. Int J Cosmet Sci 2007;29(3):147-68.

Ming X-F, Yang Z. Functions and Mechanisms of Arginase in Age-Associated Cardiovascular Diseases. Current Translational Geriatrics and Experimental Gerontology Reports 2013;2(4):268-74.

Mizutani A, Inoue H, Takeda Y. Changes in Polyamine Metabolism during Wound-Healing in Rat Skin. Biochimica et biophysica acta 1974;338(1):183-90.

Moretto J, Girard C, Demougeot C. The role of arginase in aging: A systematic review. Exp Gerontol 2019;116:54-73.

Muller I, Hailu A, Choi BS, Abebe T, Fuentes JM, Munder M, et al. Age-related alteration of arginase activity impacts on severity of leishmaniasis. PLoS Negl Trop Dis 2008;2(5):e235.

Nakajima KI, Zhu K, Sun YH, Hegyi B, Zeng Q, Murphy CJ, et al. KCNJ15/Kir4.2 couples with polyamines to sense weak extracellular electric fields in galvanotaxis. Nat Commun 2015;6(1):8532.

Ochoa JB, Strange J, Kearney P, Gellin G, Endean E, Fitzpatrick E. Effects of L-arginine on the proliferation of T lymphocyte subpopulations. JPEN Journal of parenteral and enteral nutrition 2001;25(1):23-9.

Pastar I, Stojadinovic O, Yin NC, Ramirez H, Nusbaum AG, Sawaya A, et al. Epithelialization in Wound Healing: A Comprehensive Review. Advances in wound care 2014;3(7):445-64.

Pegg AE, McCann PP. Polyamine metabolism and function. Am J Physiol 1982;243(5):C212-21.

Pietila M, Pirinen E, Keskitalo S, Juutinen S, Pasonen-Seppanen S, Keinanen T, et al. Disturbed keratinocyte differentiation in transgenic mice and organotypic keratinocyte cultures as a result of spermidine/spermine N-acetyltransferase overexpression. J Invest Dermatol 2005;124(3):596-601.

Ramírez-Zamora S, Méndez-Rodríguez ML, Olguín-Martínez M, Sánchez-Sevilla L, Quintana-Quintana M, García-García N, et al. Increased erythrocytes by-products of arginine catabolism are associated with hyperglycemia and could be involved in the pathogenesis of type 2 diabetes mellitus. Plos One 2013;8(6):e66823-e.

Ramot Y, Tiede S, Biro T, Abu Bakar MH, Sugawara K, Philpott MP, et al. Spermidine Promotes Human Hair Growth and Is a Novel Modulator of Human Epithelial Stem Cell Functions. Plos One 2011;6(7).

Shi HP, Fishel RS, Efron DT, Williams JZ, Fishel MH, Barbul A. Effect of supplemental ornithine on wound healing. J Surg Res 2002;106(2):299-302.

Sindrilaru A, Peters T, Wieschalka S, Baican C, Baican A, Peter H, et al. An unrestrained proinflammatory M1 macrophage population induced by iron impairs wound healing in humans and mice. The Journal of clinical investigation 2011;121(3):985-97.

Stojadinovic O, Brem H, Vouthounis C, Lee B, Fallon J, Stallcup M, et al. Molecular pathogenesis of chronic wounds: the role of beta-catenin and c-myc in the inhibition of epithelialization and wound healing. Am J Pathol 2005;167(1):59-69.

Stojadinovic O, Pastar I, Vukelic S, Mahoney MG, Brennan D, Krzyzanowska A, et al. Deregulation of keratinocyte differentiation and activation: a hallmark of venous ulcers. Journal of cellular and molecular medicine 2008;12(6B):2675-90.

Stojadinovic OS, Tomic-Canic M. Chapter 14 Human Ex Vivo Wound Healing Model. In: Gourdie RG, Myers TA, editors. Wound Regeneration and Repair: Methods and Protocols. Totowa, NJ: Humana Press; 2013. p. E1-E.

Tai G, Tai M, Zhao M. Electrically stimulated cell migration and its contribution to wound healing. Burns Trauma 2018;6:20.

Thomason HA, Cooper NH, Ansell DM, Chiu M, Merrit AJ, Hardman MJ, et al. Direct evidence that PKCalpha positively regulates wound re-epithelialization: correlation with changes in desmosomal adhesiveness. J Pathol 2012;227(3):346-56.

Tong BC, Barbul A. Cellular and physiological effects of arginine. Mini reviews in medicinal chemistry 2004;4(8):823-32.

Wallace HM, Mackarel AJ. Regulation of polyamine acetylation and efflux in human cancer cells. Biochem Soc Trans 1998;26(4):571-5.

Wessagowit V, Mallipeddi R, McGrath JA, South AP. Altered expression of L-arginine metabolism pathway genes in chronic wounds in recessive dystrophic epidermolysis bullosa. Clin Exp Dermatol 2004;29(6):664-8.

Williams H, Campbell L, Crompton RA, Singh G, McHugh BJ, Davidson DJ, et al. Microbial Host Interactions and Impaired Wound Healing in Mice and Humans: Defining a Role for BD14 and NOD2. J Invest Dermatol 2018;138(10):2264-74.

Witte MB, Barbul A, Schick MA, Vogt N, Becker HD. Upregulation of arginase expression in wound-derived fibroblasts. J Surg Res 2002;105(1):35-42.

Wu G, Morris SM, Jr. Arginine metabolism: nitric oxide and beyond. Biochem J 1998;336 (Pt 1)(1):1-17.

FIGURE LEGENDS

Figure 1. Temporal epidermal arginase1 expression during cutaneous wound repair. (a) Representative IHC arginase1 staining of acute human (dashed line indicates basement membrane) and (b) mouse day 3 incisional wounds. Scale bar = 400μm (zoomed image 100μm). (c) Quantification and (d) representative IF staining of epidermal arginase1 expression in acute murine incisional wounds, yellow arrows indicate arginase1 epidermal staining. Keratin 14 shows the epidermal layers of the skin. White arrows indicate the dermal wound edge and white dashed lines outline the basement membrane (Red=K14; Green=Arginase1; Blue=Dapi; Scale bar = 50μm; n=4 or 6 human wounds or mice/group respectively).

Figure 2. Epidermal arginase1 expression is reduced in impaired healing. (a) Representative IHC arginase1 expression from young intact and ovariectomized (ovx) 3day murine wounds (Scale=100μm) and (b) quantification. (c) Epidermal arginase1 expression in aged versus young murine wounds at 3days post-wounding. Yellow arrows indicate arginase1 epidermal staining; white arrows the wound edge (Scale=50μm; n=5 mice/group). (d) Quantification of epidermal arginase1 expression in aged versus young 3day wounds. (e) Human DFUs obtained at presentation were analysed for arginase1 expression then grouped by length of time to heal (Healed <8weeks; Non-Healed >12weeks from initial visit). Arginase1 expression was quantified in healed and non-healed DFUs (f) and representative staining is shown in (g; Scale=50μm). Mean±SEM; n=6 patients with healed wounds and n=13 non-healed wounds; Red=K14; Green=Arginase1; Blue=Dapi; dashed white lines outline basement membrane; unpaired t-test (b,d,f).

Figure 3. Epidermal arginase1 is essential for timely healing. (a) Representative arginase1 IHC staining of 3day wounds from *K14cre;Arg1*$^{wt/wt}$ and *K14cre;Arg1*$^{fl/fl}$ C57BL/6 mice (solid black arrows indicate epidermal arginase1 stain; open arrows indicate dermal arginase1 positive cells; dashed lines outline the basement membrane (Scale=50μm neo-epidermis, 200μm full wound). (b) Quantification of whole wound temporal arginase activity. (c) Representative H+E sections of *K14cre;Arg1*$^{wt/wt}$ and *K14cre;Arg1*$^{fl/fl}$ 3day incisional wounds (dashed lines indicate wound margins; scale=250μm) and (d) wound area quantification. (e) Representative K14 staining of 3day wounds (solid lines indicate degree of epidermal closure, dashed lines indicate the path to re-epithelialization, scale=200μm) and (f) quantification of re-epithelialization. (g) Microarray analysis of neo-epidermal gene transcriptional profiles between *K14cre;Arg1*$^{fl/fl}$ and *K14cre;Arg1*$^{wt/wt}$ wounds. Mean±SEM; n=4-6 mice/group; *p<0.05; ordinary two-way ANOVA with Sidaks multiple comparisons (b, d), Mann-Whitney U (f).

Figure 4. Arginase1 is important in regulation of epidermal activation and proliferation. (a) Representative K6 IHC staining of *K14cre;Arg1*$^{wt/wt}$ and *K14cre;Arg1*$^{fl/fl}$ wounds at 3days post-wounding. Open arrows indicate the wound edge; solidarrows indicate the cessation of K6 expression (Scale=100μm). Enumeration of K6 (b) distance from wound edge and (c) neo-epidermal expression. (d) Representative Ki67 staining of *K14cre;Arg1*$^{wt/wt}$ and *K14cre;Arg1*$^{fl/fl}$ wounds, illustrating the neo-epidermis (scale=50μm) and the wound edge (500μm distance from black arrow, scale=20μm) at 3days post-wounding and the peri-wound edge (500-1000μm from black arrow, scale=20μm) at 7days post-wounding. (e) Quantification of neo-epidermal proliferation and (f) proliferating, Ki67 positive, basal keratinocytes extending from the (g) wound edge and (h) peri-wound edge. Mean±SEM;

n=5-6 mice/group; *p<0.05; Mann-Whitney U (b-c), or *p<0.05, **p<0.01, ***p<0.001; ordinary two-way ANOVA with Sidak's multiple comparison (e-h).

Figure 5. Arginase1 is important in regulation of epidermal differentiation. (a) Representative IF illustrating co-localization (arrowed) of arginase1 and differentiation markers K10, filaggrin and loricrin at the epidermal wound edge of *K14cre;Arg1*$^{wt/wt}$ control mice at 5days post-wounding (Red=Keratin10/Filaggrin/Loricrin; Green=Arginase1; Blue=Dapi) (Scale=50µm; dashed lines outline the basement membrane). (b) qPCR of differentiated *in vitro* human keratinocytes showing *ARG1 (<0.05)* upregulation in line with differentiation markers *KRT10, FLG* and*LOR.* (c) Representative images ofdifferentiation markers K10 and loricrin in 7day *K14cre;Arg1*$^{wt/wt}$ and *K14cre;Arg1*$^{fl/fl}$ wounds (Scale=100µm) and their respective quantification (d, e) . Mean ± SEM; n = 5-6 mice/group; *p<0.05; repeated measures (b) or Mann-Whitney U (d-e).

Figure 6. Manipulating the balance of arginase activity restores healing in human models of cutaneous repair. (a) Representative *in vitro* keratinocyte (N/TERT-1) wound closure images, 10 hours post scratch, treated with arginase inhibitor nor-NOHA (5µM) and/or putrescine (10µM) with (b) quantification of percentage wound closure. (v) Quantification of wound closure of nor-NOHA (10µM) and/or Putrescine (100µM) treated human skin explants, 3days post-wounding with.(d) representative images wholemount stained with K14. Mean ± SEM; n = 5-7/group; *p<0.05, **p<0.01, ***p<0.001 vs control; repeated measures two-way ANOVA with Sidak's multiple comparisons (b) or ordinary one-way ANOVA with Tukey's multiple comparisons (c).

Supplementary Figure S1. Arginase1 expression in unwounded murine skin. Representative epidermal arginase1 expression in unwounded C57BL/6 mouse skin (dashed line indicates basement membrane; Scale bar = 10μm; n=2).

Supplementary Figure S2. Epidermal arginase1 expression in age associated delayed murine healing. Epidermal arginase1 expression in an aged (18 months) versus young (7 weeks) murine incisional wound model of delayed healing at 3 days post wounding. Single colour images of Figure 2C. Yellow arrows indicate arginase1 positive epidermal staining. White arrows indicate the wound edge and dashed white lines outline the basement membrane (Red=K14; Green=Arginase1; Blue=Dapi; Scale bar = 50μm; n=5 mice/group).

Supplementary Figure S3. Normal skin phenotype of epidermal arginase1 depleted mice. Representative H+E (scale = 100μm) and IHC stained (keratin 14; keratin 10; loricrin; keratin 6; Ki67; (scale = 50μm) and TUNEL (scale = 20μm) images of K14cre;Arg1wt/wt and K14cre;Arg1fl/fl normal skin; n= 5 mice/group.

Supplementary Figure S4. Wound immune response to epidermal arginase1 deletion. Quantification of (A) neutrophils, (B) macrophages and (C) arginase1 expressing dermal cells over a time course of 3 and 7 days post wounding reveals an altered immune response in K14cre;Arg1fl/fl wounds compared to K14cre;Arg1wt/wt control wounds. (D-F) Microarray analysis of neo-epidermal 3 day wound tissue shows alterations in immune associated gene transcription of K14cre;Arg1fl/fl wounds compared to K14cre;Arg1wt/wt control wounds. Mean+SEM; n=5-6 mice/group; **p <0.01, ***p<0.001; Mann-Whitney U (A-C).

Supplementary Figure S5. Arginase inhibition delays keratinocyte scratch closure in vitro. (A) Quantification of HaCaT temporal arginase activity, shows a trend towards a reduction in arginase activity 48 hour post scratch wounding, determined by urea production. (B) Quantification of HaCaT scratch closure following nor-NOHA treatment compared to control and (C) representative crystal-violet stained HaCaT wounds after nor-NOHA treatment (yellow line indicates migrating wound edge). Mean±SEM; n = 3/4/group; NS = ordinary one-way ANOVA with Tukey's multiple comparisons (A) or **p<0.01 Kruskal Wallis test with Dunn's multiple comparisons (B).

Supplementary Figure S6. Altered metabolism of arginine by arginase in cutaneous healing. (Graphical Abstract) (A) Normal homeostasis and wound re-epithelialisation (blue outline). (B) Inhibition of arginase allows greater NOS metabolism and reduced polyamine synthesis, leading to reduced wound edge keratinocyte proliferation and migration impacting re-epithelialisation and differentiation (red arrows). (C) Downstream activation of the arginase pathway with putrescine decreases wound closure impacting cell migration (green arrows/outline). B and C combined restores healing as A. Abbreviations; NOS _ nitric oxide synthase; NOHA _ N-hydroxy-L-arginine; Nor-NOHA - N-hydroxy-nor-arginine; NO _ nitric oxide; ODC _ ornithine decarboxylase; AMD1 - Sadenosylmethionine decarboxylase proenzyme; SPDS _ spermidine synthase; SMS _ spermine synthase; SAT1 _ diamine acetyltransferase 1; PAOX _ peroxisomal N(1)-acetyl-spermine/spermidine oxidase; SMOX _ spermine oxidase.

Supplementalry Table S1. Quantitative real-time PCR primers

Gene	Primer sequences (5'->3')		Product length (bp)
	Forward	**Reverse**	
YWHAZ	ACTTTTGGTACATTGTGGCTTCAA	CCGCCAGGACAAACCAGTAT	94
ARG1	AAGATTCCCGATGTGCCAGG	GTCCACGTCTCTCAAGCCAA	87
LOR	CTCACCCTTCCTGGTGCTTT	GGGTGGGCTGCTTTTTCTGA	73
K10	TCCCAACTGGCCTTGAAACA	TGAGAGCTGCACACAGTAGC	75
FLG	CAGGCTCCTTCAGGCTACATT	GCAAAGATGTTTTCCAGGAGAGT	95
FLG2	GCAAGCTGCATCAGGCTTTA	CACTTCTCAAGAGGTCGGTCA	90

Supplementary Table S2. IHC and IF primary antibodies

Primary Antibody	Product Number	Company
anti-liver arginase goat polyclonal	ab92274	Abcam, Cambridge, UK
anti-arginase1-I goat polyclonal	SC-18354	Santa Cruz Biotechnology, Heidelberg, Germany
anti-NOS2 rabbit polyclonal	SC-651	Santa Cruz Biotechnology, Heidelberg, Germany
anti-keratin6 rabbit polyclonal	PRB-169P	Covance, Maidenhead, UK
anti-keratin14 rabbit polyclonal	PRB-155P	Covance, Maidenhead, UK
anti-loricrin rabbit polyclonal	PRB-145P	Covance, Maidenhead, UK
anti-keratin10 rabbit polyclonal	905404	Biolegend, CA, USA
anti-filaggrin rabbit polyclonal	Ab24584	Abcam, Cambridge, UK
anti-Ki67 rabbit monoclonal	Ab16667	Abcam, Cambridge, UK
anti-neutrophil rat polyclonal	MA1-40038	ThermoFisher Scientific, Loughborough, UK
anti-Mac-3 rat polyclonal	553322	BD Biosciences, Oxford, UK

SUPPLEMENTARY TEXT

MATERIALS AND METHODS

Human acute and chronic wounds

Acute wound samples were collected from 3 healthy volunteers (male, aged ≥30 years). Briefly, 1.5 mm punch biopsies were taken from the left upper inner arm following local 1% lignocaine infiltration. This initial biopsy was excised using a second 3 mm biopsy. Chronic wound biopsy samples were used from 19 patients (mixed sex, aged ≥40 years) with chronic DFU (defined as distal to the medial and lateral malleoli, with a known duration ≥4 weeks, grade A1/B1 according to the University of Texas ulcer classification, no infection or ischaemia at the time of presentation) as previously described. All patients received standard-of-care treatment, including regular debridement, non-anti-microbial dressings and offloading. No local anaesthetic was used at any time during treatment. At presentation, wound biopsy samples were collected from the margin of DFUs prior to debridement using sterile technique. Patients were followed for a period of 12 weeks (via weekly visits to the diabetic clinic), with photographs taken at each visit to determine longitudinal healing outcome using wound traces and calculating the wound area with ImageJ 1.x software (ImageJ, Maryland, USA). DFUs were then separated into two groups, those who healed (full wound closure at ≤7 weeks; 6 patients) and those who failed to heal (wound not closed at 12 weeks; 13 patients) following current best practice treatment. Samples were fixed and processed for histological analysis.

Conditional arginase1 knockout mouse model

Following local ethics committee approval, all animal studies were conducted in accordance with UK Home Office regulations. All mice used in this study were bred in the same room

under the same conditions at the University of Manchester's Biological Services Facility, housed in isolator cages with *ad libitum* food and water. The room was maintained at a constant temperature of 21°C, with 45-65% humidity on a 12 hour light-dark cycle. *K14-cre;Arg1*$^{fl/fl}$ mice were generated in house by crossing an arginase1 floxed mouse (El Kasmi et al., 2008) with a K14cre expressing mouse (Li M. et al., 2001) and *K14-cre;Arg1*$^{wt/wt}$ mice were used as cre positive controls (all C57BL/6J background). Transgenic mice were bred onsite from homozygous mating. Genotype was determined by PCR (see Genotyping supplemental section) and cell specific deletion confirmed by IHC. IHC results confirmed a lack of arginase1 expression in the neo-epidermal tongues of *K14cre;Arg1*$^{fl/fl}$ wounds compared to *K14cre;Arg1*$^{wt/wt}$ controls. The specificity of the knockout was also demonstrated by retained dermal arginase1 expression in *K14cre;Arg1*$^{fl/fl}$ mice (Figure 3a).

Genotyping

Mice were genotyped by PCR using three sets of primers (Invitrogen, Loughborough, UK); *arg flox* [F- TGCGAGTTCATGACTAAGGTT; R- AAAGCTCAGGTGAATCGG; wt200bp; floxed230bp]; *k14 cre* [F- ATTTGCCTGCATTACCGGTC; R- ATCAACGTTTTGTTTTCGGA; 349bp]; and deletion confirmation [F- CCCCCAAAGGAAATGTAAGAA; R- CACTGTCTAAGCCCGAGAGTA; 500bp] and HS MyTaq Red mastermix (Bioline). Reactions were performed using a SimpliAmp Thermal Cycler (Applied Biosystems, Loughborough, UK) using the following cycling parameters; Initial denaturation (95°C 3min); 40x cycles 1. Denaturation (94°C 45sec) 2. Annealing (53°C *arg flox* or 55°C delta and *k14 cre* 45sec) 3. Elongation (72°C 1min); Final extension (72°C 5min). PCR products were run on a standard 2% agarose gel (Bioline, London, UK). A single *arg flox* band; *k14 cre* band and delta band indicate the *K14cre;Arg1*$^{fl/fl}$ genotype. A

single *arg wt* band; *k14 cre* band and the absence of a delta band indicate the *K14cre;Arg1*$^{wt/wt}$ genotype.

Quantitative real-time PCR

In brief, cDNA was transcribed from 0.5µg of RNA using the GoScript RT kit (Promega, Madison, WI) and quantitative PCR performed using the PowerUp Sybr Green Master Mix (Thermo, UK) and LightCycler 480 Instrument (Roche, UK). For each primer set, an optimal dilution was determined and melt curves were used to determine amplification specificity. Each sample was performed in triplicate and relative expression was determined from a standard curve. Expression ratios were normalized to the housekeeper *YWHAZ*. Full primer sequences are listed in Supplementary Table S1.

IHC and IF image analysis

All antibodies used are listed in Supplementary Table S2. Images were acquired on a 3D-Histech Pannoramic-250 microscope slide-scanner using a 20x/ 0.80 Plan Apochromat objective (Zeiss, Cambridge, UK) and the DAPI, FITC and TRITC filter sets for fluorescence imaging. Snapshots of the slide-scans were taken using the Case Viewer software (3D-Histech). Images were also acquired using manual microscopes; a Nikon Eclipse E600 microscope and a SPOT insight camera (Image solutions Inc, Preston, UK); or a Nikon Eclipse Ci microscope using 4x/0.13; 10x/0.30; 20x/0.50 or 40x/0.75 Plan Fluor objectives, with a Nikon DS-Fi3 camera and NIS-Elements software (Nikon, Kingston Upon Thames, UK). Quantification of wound measurements and cell counts were performed using Image Pro Premier software (Media Cybernetics, Abingdon, UK) as described previously (Williams et al., 2018). Briefly, H+E stains imaged at x4 magnification were analysed for wound area,

wound width and percent re-epithelialization (confirmed with K14 stained sections). The wound area was considered the area of granulation tissue beneath the clot to the margins of normal skin either side of the wound. Percent re-epithelialization was determined by dividing the sum length of each neo-epidermal tongue by the total distance required to fully close the wound. K6 staining was quantified by area measurements of the neo-epidermal tongue and the length of K6 staining away from the wound edge, taken as an average of each side per wound. Ki67 IHC was quantified by cells/neo-epidermal area. Basal Ki67 expression was manually counted as a percentage of positive and total basal keratinocytes, measured at the wound edge (0-500µm distance from the wound edge) and the peri-wound edge (500-1000µm distance from the wound edge). Cell counts within the wound area were determined using 5 representative images of the granulation tissue at x20 magnification. Keratin 10 and Loricrin staining were quantified based on a subjective scoring system out of 10; 0 being no positive staining in the newly formed epidermis and 10 being as normal skin. Arginase1 staining was quantified, as an average score from x20 magnification images of the entire epidermis of DFU sections or neo-epidermal/wound edge regions of acute mouse wounds, based on a subjective scoring system out of 10 for both epidermal coverage (IHC) or stain intensity (IF) (0 = no expression; 10 = full coverage or high intensity). All staining and quantification was performed blind.

TUNEL staining

Briefly, rehydrated tissue sections were incubated in Proteinase K (20µg/ml proteinase K in 10mM Tris/HCl pH 7.5) for 20min at 37°C, followed by washing in PBS. Sections were incubated in TUNEL reaction mixture (1:10 Enzyme Solution: Label Solution) or Label Solution as a negative control, in the dark for 30min at 37°C. After washing, sections were counterstained with DAPI (1µg/ml) (ThermoFisher Scientific) for 5min at room temperature,

washed and mounted using Prolong Gold Antifade Mounting Media (ThermoFisher Scientific) and visualized under a fluorescent microscope.

Arginase activity assay

In brief, normal skin and wound tissue was homogenized in 0.1% Triton X-100 (Sigma). After 30min, samples were centrifuged for 1min at 8000g to pellet cell debris. Assay buffer (10mM MnCl in 50mM Tris, pH 7.5) was added to the supernatant for 10 minutes at 56°C. Samples were incubated with the arginase substrate L-arginine (0.5M L-Arginine pH9.7) for 3hrs at 37°C before adding acid stop solution (H_2SO_4 (Sigma) : H_3PO_4 (Sigma) : H_20 in 1:3:7 ratio (v/v)). 9% α-isonitrosopropiophenone (Sigma) was added and samples heated at 100°C protected from light. Absorbance was measured after 45min at 570nm (VersaMax microplate reader, Molecular Devices LLC) and urea concentration was calculated against a standard curve. Total protein concentration in the cell lysates was determined by the Pierce 660nm Protein Assay (ThermoFisher Scientific) to normalize each sample.

Laser Capture Microscopy (LCM)

Day 3 incisional wounds (n=4/group) were snap frozen upon tissue harvest and OCT embedded prior to cryosectioning. 10µm thick cryosections were obtained using a clean RNase free designated CM3050 cryostat (Leica Biosystems) and mounted onto RNase free MMI MembraneSlides, inverted and placed onto a glass slide for protection against contamination. Samples were dehydrated in isopropanol (30sec) and xylene (30sec) and air dried immediately prior to LCM. Samples were laser microdissected using the MMI CellCut laser microdissection system (Olympus, Southend-on-Sea, UK). Using the freehand tool in

the MMI software, cells of the neo-epidermis were marked and cut automatically using a 20x/0.45 Plan FL N objective and UV-Laser at 60% power; speed of 18µm/s; focal point of 350. The isolated target cells were collected from the MMI Membrane Slides by lowering and lifting of the adhesive cap of 0.5ml MMI Isolation Caps (Olympus) held from above. Captured samples were stored in Lysis Solution (Ambion RNAqueous-Micro Kit component) inverted on ice then stored at -80°C until ready for RNA isolation.

Microarray

Data was provided to the Bioinformatics core facility in the Faculty of Biology Medicine and Health, University of Manchester, for analysis as follows. Technical quality control and outlier analysis was performed with dChip (V2005) (Li and Wong, 2001) using the default settings. Mouse Transcriptome Assay 1.0 data were processed and analysed using Partek Genomics Solution (version 6.6, Copyright 2009, Partek Inc., St. Charles, MO, USA) with the following options: probesets were quantile normalized and RMA background correction applied. Probesets were summarized to genes by calculating the means (log 2). Validation and gene enrichment strategies consisted of the following steps. Step 1, to establish relationships and compare variability between replicate arrays and experimental conditions, principal components analysis (PCA) was used. PCA was chosen for its ability to reduce the effective dimensionality of complex gene-expression space without significant loss of information (Quackenbush, 2001). Step 2, Differential expression analysis was performed on annotated genes with Limma using the functions lmFit and eBayes (Smyth, 2004). Gene lists of differentially expressed genes were controlled for false discovery rate (fdr) errors using the Benjamini–Hochberg procedure (Team, 2008). Step 3, functional annotation of gene lists containing significantly differentially expressed genes was done with QIAGEN's Ingenuity Pathway Analysis (IPA®, QIAGEN Redwood City, www.qiagen.com/ingenuity), filtered to

fold change +/-1.25 and p value <0.05. Supplemental data presented is unfiltered by fold change with a p value <0.05. Raw data was deposited in ArrayExpress (accession number: E-MTAB-10213).

In vitro cell analysis

Keratinocyte culture

Normal human epidermal keratinocytes (NHEKs) isolated from juvenile foreskin (Promocell) were cultured in keratinocyte growth medium 2 (Promocell) at 37°C with 5% CO_2. NHEKs were used in experiments at P3-5. N/TERT-1 cells were cultured at 37°C with 5% CO_2 in Keratinocyte Serum Free Media (Complete KSFM: low Ca2+ (500µl of 300mM) K-SFM (with 25µg/ml BPE, 0.2ng/ml EGF, 5ml Pen/Strep) and transferred to DFK-2 media (50:50 ratio of DFK-1 media (DMEM (high glucose), F-12 , 25µg/ml BPE, 0.2ng/ml EGF, 5ml L-glutamine, 5ml Pen/Strep) and K-SFM,all from GIBCO). HaCaT cells (ATCC12191) were cultured in DMEM (high glucose) with 10% FBS and 1x Pen/Strep at 37°C with 5% CO_2.

Human skin wound explant model

Briefly, adult female abdominal skin (Caucasian, aged ≥50 years from four donors) was washed in sterile PBS and excess fat removed. 3mm partial thickness wounds were generated within 8mm diameter biopsy-punched constructs. Biopsies were cultured within 6well plates, placed on a stack, consisting of a 0.45µm nylon membrane on top of 2x absorbent pads, saturated with 1ml of Williams E media + supplements (100U Penicillin and 0.1mg Streptomycin per ml, 2mM l-glutamine, 10µg/ml insulin, 10ng/ml hydrocortisone (Sigma)). 10µl nor-NOHA 10µM (Cayman, Michigan, USA) or Putrescine 100µM (Sigma) was applied directly to the wound. Biopsies were maintained at 37°C, 5% CO_2 for 3 days, media replenished and re-treated daily, then formalin fixed before wholemount staining with anti-

keratin 14 antibody. Images were obtained using a stereo microscope (Leica) and camera (Leica) and wound re-epithelialization was determined by calculating the remaining wound area as a percentage of the initial wound area, measured using Image Pro Premier software (Media Cybernetics, Abingdon, UK).

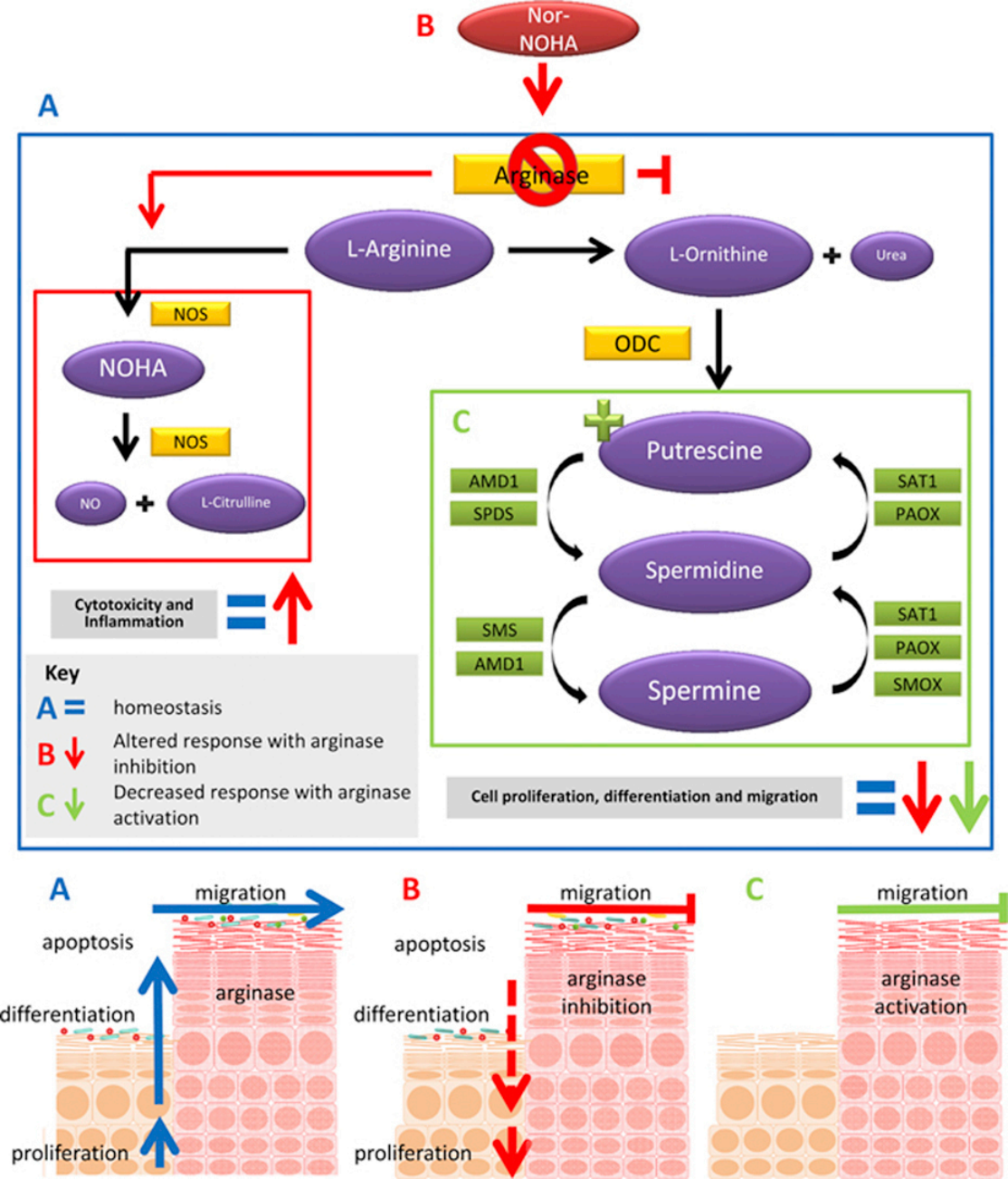
B
Nor-NOHA
A
Arginase
L-Arginine
L-Ornithine
Urea
NOS
NOHA
NOS
NO
L-Citrulline
ODC
C
Putrescine
AMD1
SPDS
SAT1
PAOX
Spermidine
SMS
AMD1
SAT1
PAOX
SMOX
Spermine
Cytotoxicity and Inflammation
Cell proliferation, differentiation and migration
Key
A = homeostasis
B ↓ Altered response with arginase inhibition
C ↓ Decreased response with arginase activation
A
migration
apoptosis
arginase
differentiation
proliferation
B
migration
apoptosis
arginase inhibition
differentiation
proliferation
C
migration
arginase activation

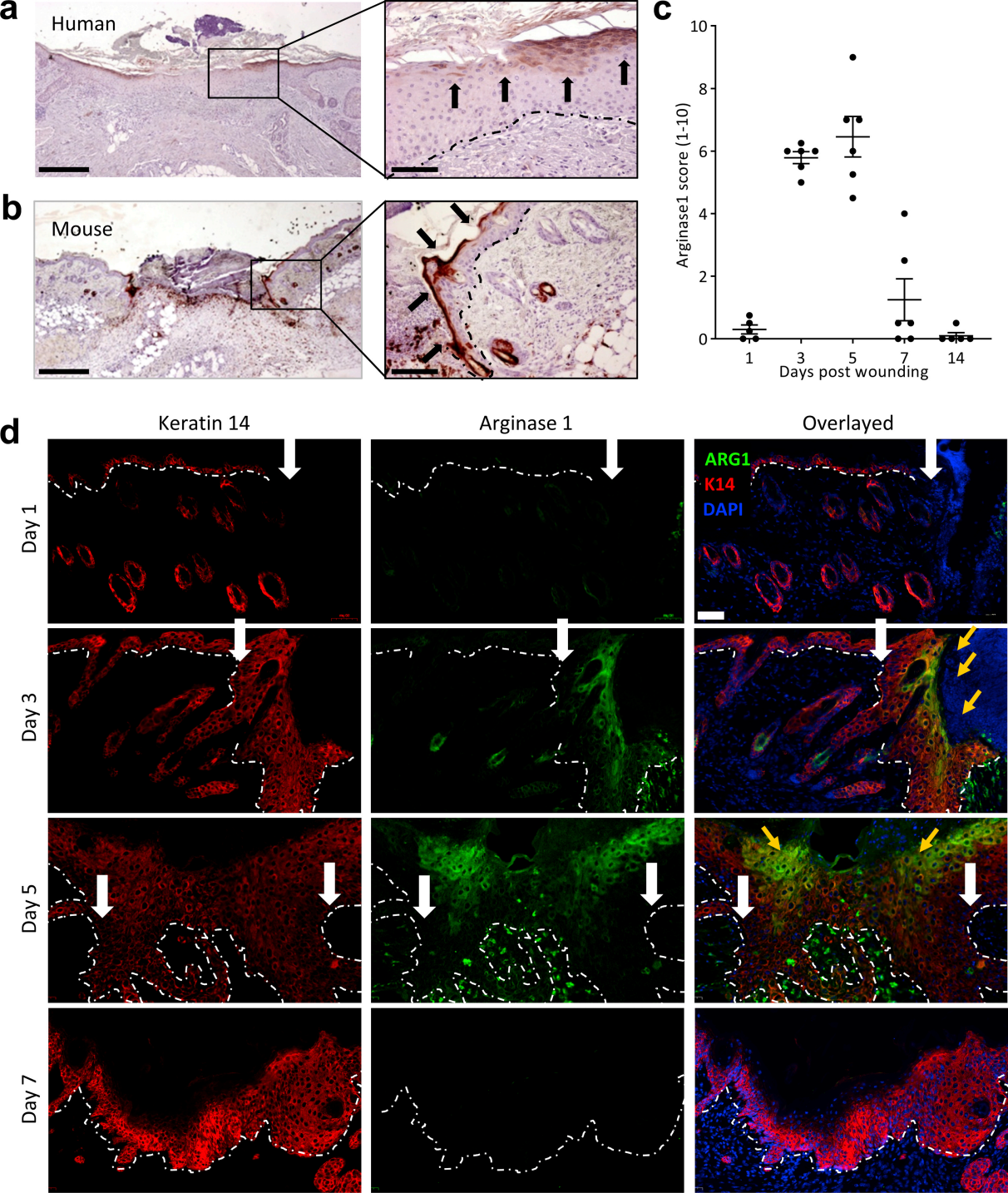
a
Human
b
Mouse
c
Arginase1 score (1-10)
10
8
6
4
2
0
1
3
5
7
14
Days post wounding
d
Keratin 14
Arginase 1
Overlayed
ARG1
K14
DAPI
Day 1
Day 3
Day 5
Day 7

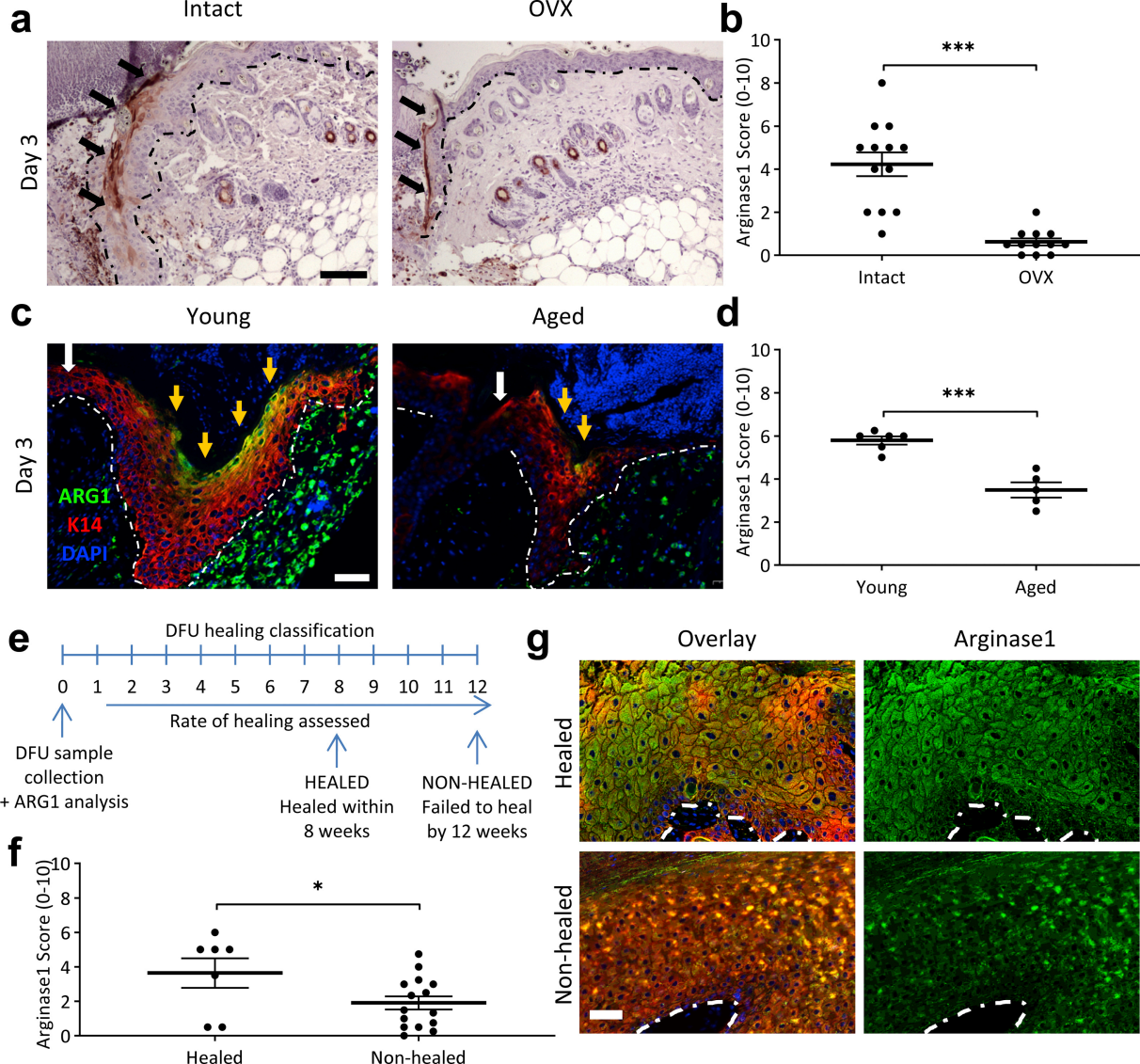
a
Intact
OVX
Day 3
b
Arginase1 Score (0-10)
***
Intact
OVX
c
Young
Aged
Day 3
ARG1
K14
DAPI
d
Arginase1 Score (0-10)
***
Young
Aged
e
DFU healing classification
0 1 2 3 4 5 6 7 8 9 10 11 12
Rate of healing assessed
DFU sample collection + ARG1 analysis
HEALED Healed within 8 weeks
NON-HEALED Failed to heal by 12 weeks
f
Arginase1 Score (0-10)
*
Healed
Non-healed
g
Overlay
Arginase1
Healed
Non-healed

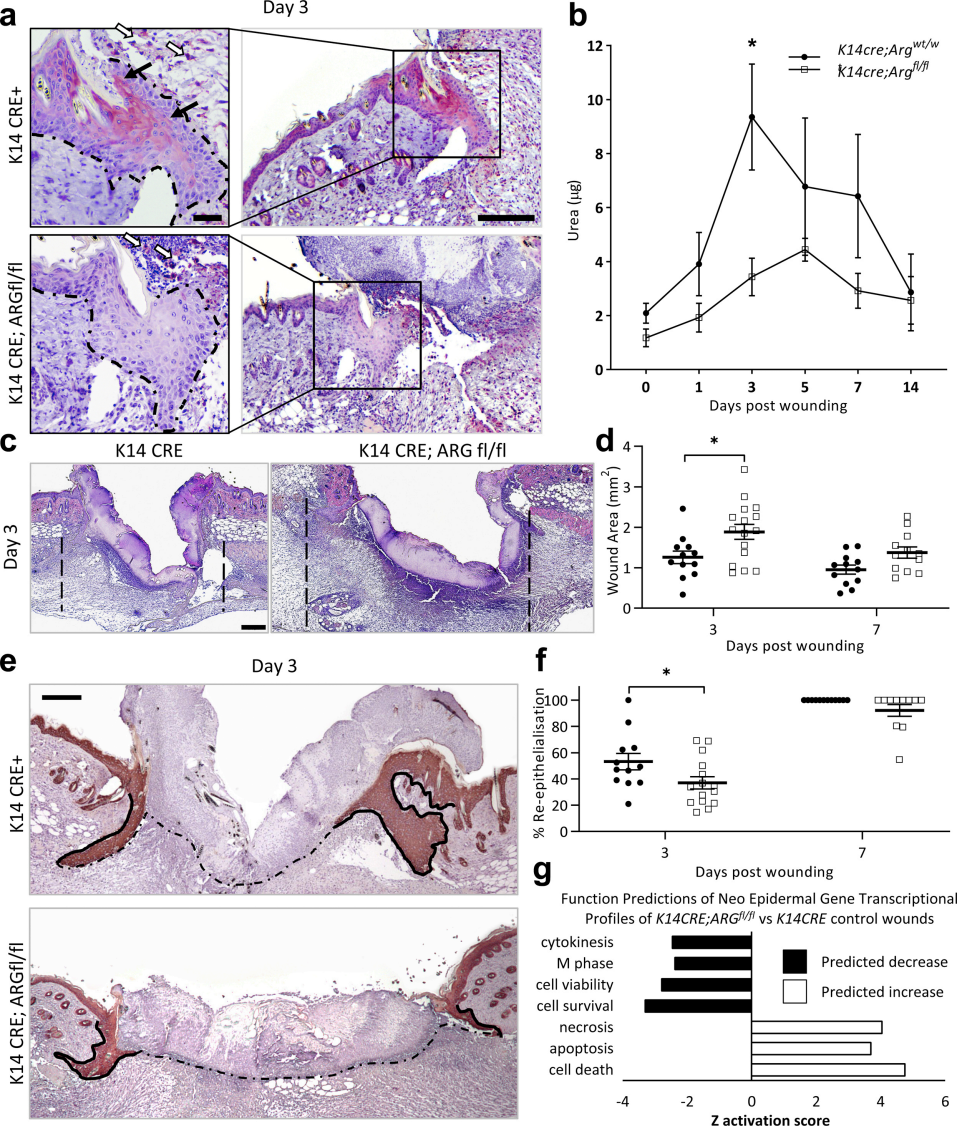
a
Day 3
K14 CRE+
K14 CRE; ARGfl/fl
b
*
K14cre;Arg^wt/w
K14cre;Arg^fl/fl
Urea (µg)
0
2
4
6
8
10
12
0
1
3
5
7
14
Days post wounding
c
K14 CRE
K14 CRE; ARG fl/fl
Day 3
d
*
Wound Area (mm^2)
0
1
2
3
4
3
7
Days post wounding
e
Day 3
K14 CRE+
K14 CRE; ARGfl/fl
f
*
% Re-epithelialisation
0
20
40
60
80
100
3
7
Days post wounding
g
Function Predictions of Neo Epidermal Gene Transcriptional Profiles of K14CRE;ARG^fl/fl vs K14CRE control wounds
cytokinesis
M phase
cell viability
cell survival
necrosis
apoptosis
cell death
Predicted decrease
Predicted increase
-4
-2
0
2
4
6
Z activation score

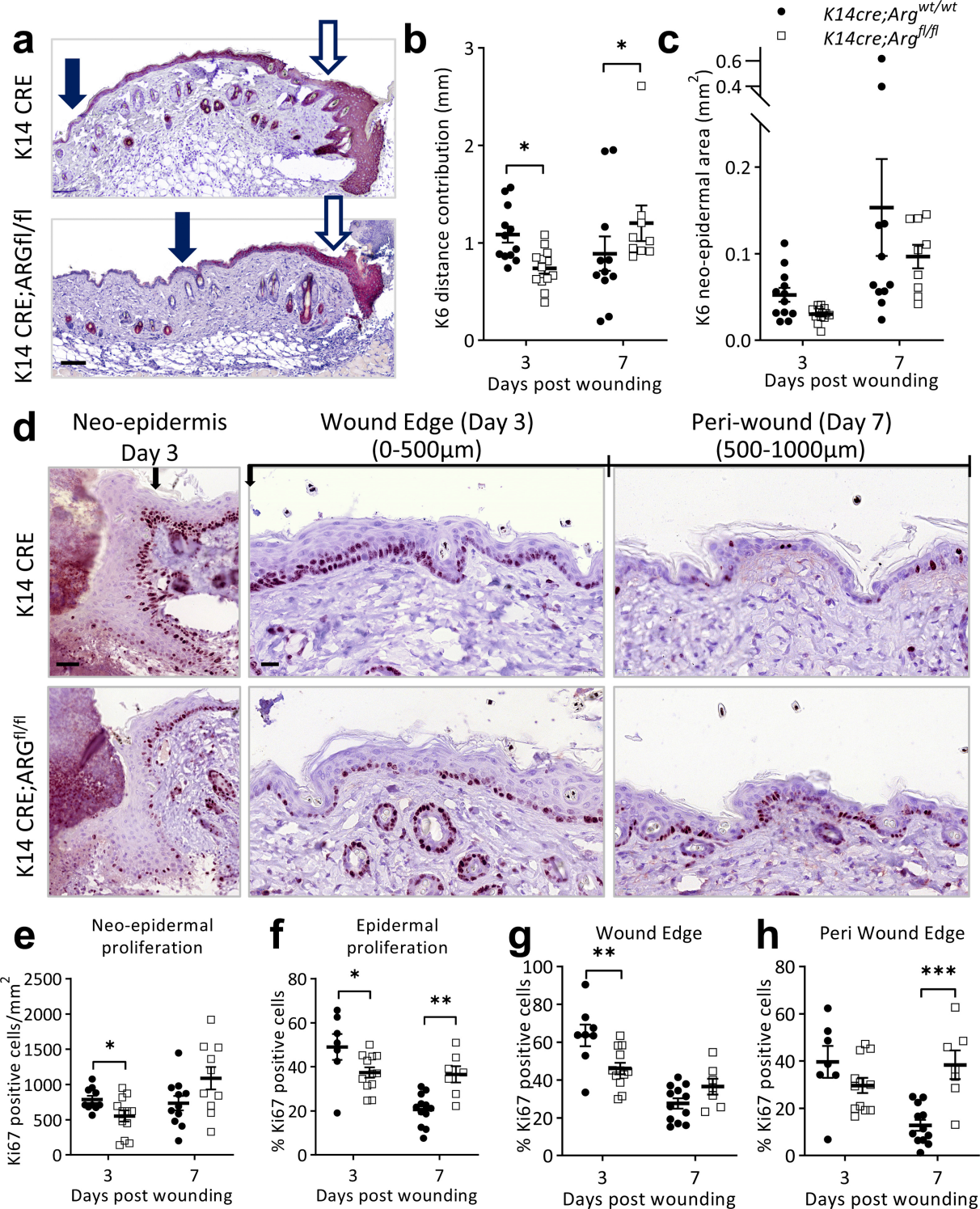
a
K14 CRE
K14 CRE;ARGfl/fl
b
K6 distance contribution (mm)
Days post wounding
c
K14cre;Arg wt/wt
K14cre;Arg fl/fl
K6 neo-epidermal area (mm2)
Days post wounding
d
Neo-epidermis Day 3
Wound Edge (Day 3) (0-500µm)
Peri-wound (Day 7) (500-1000µm)
K14 CRE
K14 CRE;ARGfl/fl
e
Neo-epidermal proliferation
Ki67 positive cells/mm2
Days post wounding
f
Epidermal proliferation
% Ki67 positive cells
Days post wounding
g
Wound Edge
% Ki67 positive cells
Days post wounding
h
Peri Wound Edge
% Ki67 positive cells
Days post wounding

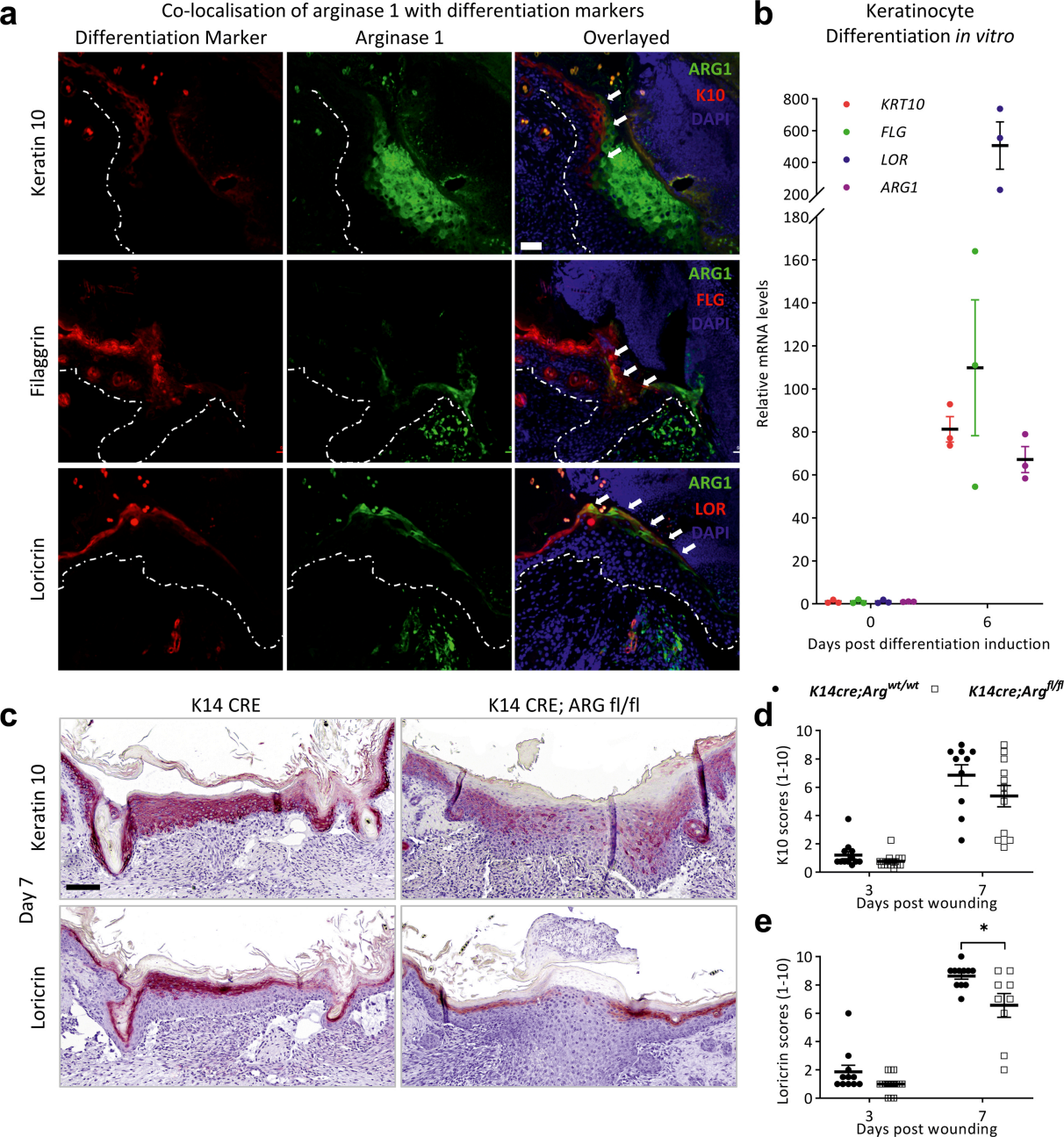
a
Co-localisation of arginase 1 with differentiation markers
Differentiation Marker
Arginase 1
Overlayed
Keratin 10
Filaggrin
Loricrin
ARG1
K10
FLG
LOR
DAPI
b
Keratinocyte
Differentiation in vitro
KRT10
FLG
LOR
ARG1
Relative mRNA levels
Days post differentiation induction
c
K14 CRE
K14 CRE; ARG fl/fl
Keratin 10
Loricrin
Day 7
K14cre;Arg wt/wt
K14cre;Arg fl/fl
d
K10 scores (1-10)
Days post wounding
e
Loricrin scores (1-10)
Days post wounding